
This is an electronic reprint of the original article.
This reprint may differ from the original in pagination and typographic detail.

Author(s): Kokkonen, Kimmo & Pensala, Tuomas & Meltaus, Johanna & Kaivola, Matti

Title: Extraction of lateral eigenmode properties in thin film bulk acoustic wave resonator from interferometric measurements

Year: 2010

Version: Final published version

Please cite the original version:

Kokkonen, Kimmo & Pensala, Tuomas & Meltaus, Johanna & Kaivola, Matti. 2010. Extraction of lateral eigenmode properties in thin film bulk acoustic wave resonator from interferometric measurements. Applied Physics Letters. Volume 96, Issue 17. 173502. ISSN 0003-6951 (printed). DOI: 10.1063/1.3299012.

Rights: © 2010 American Institute of Physics (AIP). This article may be downloaded for personal use only. Any other use requires prior permission of the author and the American Institute of Physics.
<http://scitation.aip.org/content/aip/journal/apl>

All material supplied via Aaltodoc is protected by copyright and other intellectual property rights, and duplication or sale of all or part of any of the repository collections is not permitted, except that material may be duplicated by you for your research use or educational purposes in electronic or print form. You must obtain permission for any other use. Electronic or print copies may not be offered, whether for sale or otherwise to anyone who is not an authorised user.

Extraction of lateral eigenmode properties in thin film bulk acoustic wave resonator from interferometric measurements

Kimmo Kokkonen, Tuomas Pensala, Johanna Meltaus, and Matti Kaivola

Citation: *Applied Physics Letters* **96**, 173502 (2010); doi: 10.1063/1.3299012

View online: <http://dx.doi.org/10.1063/1.3299012>

View Table of Contents: <http://scitation.aip.org/content/aip/journal/apl/96/17?ver=pdfcov>

Published by the [AIP Publishing](#)

Articles you may be interested in

[Selective normal mode excitation in multilayer thin film bulk acoustic wave resonators](#)

Appl. Phys. Lett. **105**, 162910 (2014); 10.1063/1.4899067

[Intrinsically switchable thin film bulk acoustic wave resonators](#)

Appl. Phys. Lett. **104**, 222905 (2014); 10.1063/1.4881141

[Effect of interface roughness on acoustic loss in tunable thin film bulk acoustic wave resonators](#)

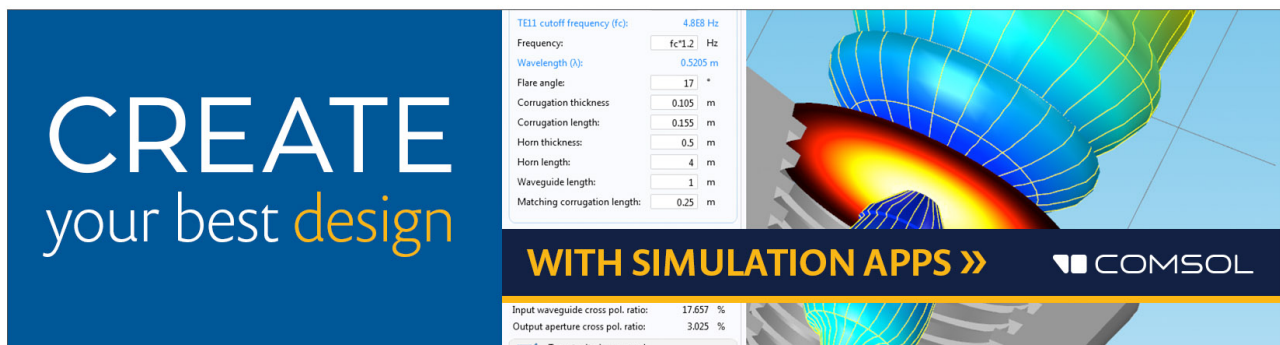
J. Appl. Phys. **110**, 024116 (2011); 10.1063/1.3610513

[Shear mode bulk acoustic wave resonator based on c-axis oriented AlN thin film](#)

J. Appl. Phys. **104**, 084508 (2008); 10.1063/1.2996319

[Laser Acoustic Imaging of Film Bulk Acoustic Resonator \(FBAR\) Lateral Mode Dispersion](#)

AIP Conf. Proc. **760**, 251 (2005); 10.1063/1.1916685

The advertisement features a blue background on the left with the text "CREATE your best design" in white and yellow. On the right, there is a 3D simulation of a horn-shaped acoustic resonator with a color gradient from blue to red. A control panel on the left lists parameters: TELL cutoff frequency (fc): 4.868 Hz; Frequency: fc*1.2 Hz; Wavelength (lambda): 0.5205 m; Flare angle: 17 degrees; Corrugation thickness: 0.105 m; Corrugation length: 0.155 m; Horn thickness: 0.5 m; Horn length: 4 m; Waveguide length: 1 m; Matching corrugation length: 0.25 m. Below the simulation, it says "WITH SIMULATION APPS >>" and the COMSOL logo. At the bottom, it shows "Input waveguide cross pol. ratio: 17.657 %", "Output aperture cross pol. ratio: 3.025 %", and a checked box for "Target criterion: passed".

Extraction of lateral eigenmode properties in thin film bulk acoustic wave resonator from interferometric measurements

Kimmo Kokkonen,^{1,a)} Tuomas Pensala,² Johanna Meltaus,² and Matti Kaivola¹

¹Department of Applied Physics, Helsinki University of Technology, Espoo 02150, Finland

²VTT Technical Research Centre of Finland, P. O. Box 1000, 02044 VTT, Finland

(Received 15 September 2009; accepted 6 January 2010; published online 26 April 2010)

A heterodyne laser interferometer is used to study acoustic wave fields excited in a 1.8 GHz AlN thin film bulk acoustic wave resonator. The electrical response of the resonator exhibits a strong thickness resonance onto which spurious modes, caused by lateral standing plate waves, are superposed. Optical interferometer measurements are used to extract dispersion curves of the laterally propagating waves responsible for the spurious responses. A discrete eigenmode spectrum due to the finite lateral dimensions of the resonator is observed. An equivalent circuit model for a multimode resonator is fitted to the mechanical resonator response extracted along a single curve in the dispersion diagram, and is used to determine properties, such as Q -values, of the individual lateral eigenmodes. Measured wave field images, extracted dispersion curves, and the eigenmode spectrum with the model fitting results are presented. © 2010 American Institute of Physics. [doi:10.1063/1.3299012]

Laser interferometry is a versatile, noncontact optical method that provides direct information on the mechanical wave fields excited in microacoustic structures. Optical probing of gigahertz-range bulk-acoustic waves (BAWs)¹⁻⁷ has proven to be very useful for studying the operation of BAW devices, revealing their loss mechanisms, helping to refine simulation models and for obtaining materials parameters. The fields can be measured with a lateral resolution better than 1 μm and with smallest detectable vibration amplitudes in the subpicometer range.

The so-called solidly mounted resonator under study here is composed of a piezoelectric thin film sandwiched between metal electrodes and of an acoustic Bragg reflector that serves to acoustically isolate the device from the substrate. The resonator operates in the lowest order longitudinal thickness (LT_1) mode, in which about half an acoustic wavelength is contained within the thickness formed by the piezoelectric film and the metal electrodes. Since the LT_1 mode can also propagate horizontally as a plate wave, standing waves are formed within the laterally finite-sized resonator. These lateral eigenmodes induce ripple in the electrical response near the main resonance. For use in frequency control applications and in filtering, effective suppression of these spurious electrical responses is desired. Therefore, the properties of the lateral eigenresonances are of great interest, to enable deeper understanding of the device physics and to further develop modeling.⁸⁻¹¹

In this letter, extraction of detailed information on individual lateral eigenmodes from the measured acoustical response is demonstrated. We present interferometric measurements of the acoustic wave fields on a 1.8 GHz AlN thin film BAW resonator. Plate wave dispersion curves are calculated from the measured wave fields, and the vibration amplitudes extracted along the LT_1 dispersion curve are presented as a function of frequency. Individual resonances are character-

ized by fitting a mechanical resonator equivalent circuit model to the measured vibration data.

The experimental method is demonstrated with a 1820 MHz AlN based resonator utilizing an acoustic reflector consisting of five alternating layers of W and SiO_2 for substrate isolation. The reflector is optimized for high Q according to the method of Marksteiner *et al.*¹² and for obtaining a desired type of plate wave dispersion¹³ to ensure lateral energy trapping. The resonator structure is schematically presented in

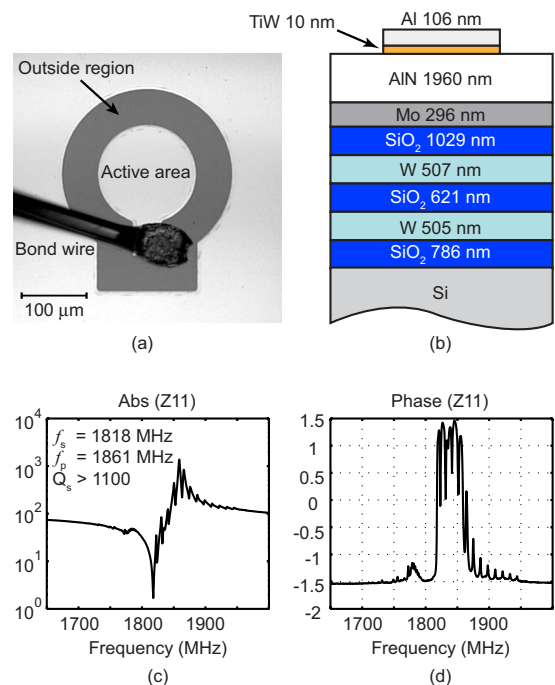


FIG. 1. (Color online) (a) Microscope image of the sample wire-bonded to a jig for interferometric measurements. (b) Schematic cross sectional view of the layer stack of the sample with measured layer thicknesses (SEM). [(c) and (d)] Magnitude and phase of impedance obtained with wafer level measurement. Main figures of merit are provided as an inset in (c). The electrical response features spurious resonances.

^{a)}Electronic mail: Kimmo.Kokkonen@tkk.fi.

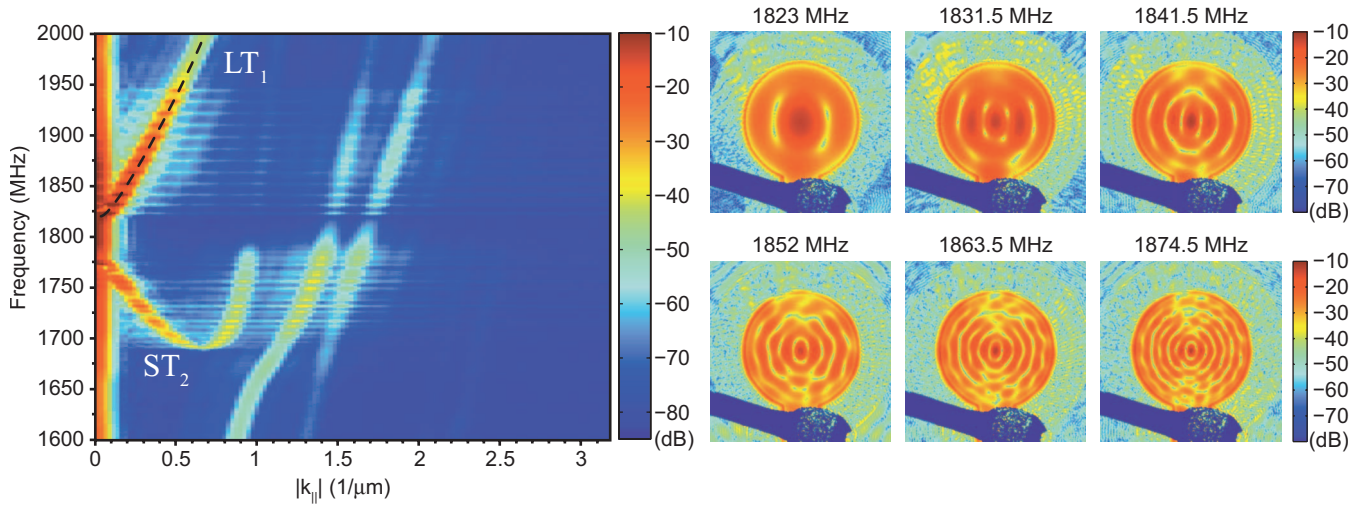


FIG. 2. (Color) Dispersion diagram calculated from the measured vibration data and measured amplitude distributions most closely corresponding to the fitted 6 first eigenfrequencies. Due to the finite lateral dimensions and high- Q resonances, the LT_1 dispersion curve (marked with dashed black line) is seen in the dispersion diagram as a chain of discrete maxima.

Fig. 1, along with a photograph and an electrical response measured on wafer. The electrical response features a strong resonance-antiresonance behavior, onto which sharp spurious oscillations are superposed, making direct extraction of the electrical figures of merit for the main resonance difficult. Approximate values are indicated in Fig. 1.

Interferometric measurements of the resonator were carried out with a scanning heterodyne laser interferometer.⁵ The heterodyne concept enables acquisition of the absolute amplitude of the surface vibration independently of the local optical surface reflectance. The heterodyne signal also carries phase information of the acoustic wave field, measured simultaneously with the amplitude data at each measurement point.

The wave field measurements feature an area of $248.49 \times 248.49 \mu\text{m}^2$, including the circular active area of the resonator and some outer region. A lateral scan step of $0.99 \mu\text{m}$ was used, resulting in scans of 252×252 (63 504) data points. In order to study the acoustic frequency response in detail, the interferometer measurements were carried out at frequencies ranging from 1600 to 2000 MHz. The frequency range was covered using three different frequency steps: a step of 1 MHz between 1600–1800 MHz and 1950–2000 MHz, 0.5 MHz between 1800–1815 MHz and 1860–1950 MHz, and a finer 0.25 MHz step between 1815–1860 MHz in order to provide better resolution near the resonance frequency f_s and the frequencies of the first LT_1 eigenmodes. The sample was driven with a nominal input power of +5 dBm from a 50Ω transmission line.

Carrying out interferometric measurements at a number of frequencies allows us to apply Fourier transform techniques to the measured wave fields at each frequency and thereby to determine the mode spectrum of the resonator as a function of frequency and present it as a plate wave dispersion diagram.^{6,14–17} The measured dispersion diagram is shown in Fig. 2. The LT_1 -dispersion curve is identified as the bright red curve emerging at just above 1820 MHz, for which the frequency increases monotonically with the lateral wave number ($k_{||}$). For a simulation of the dispersion properties, see Ref. 18. Furthermore, quantization of the LT_1 wave into lateral high- Q eigenmodes due to the finite lateral

size of the resonator results in a chain of discrete maxima seen along the dispersion curve. The lower bright red curve is identified as the second harmonic shear thickness mode (ST_2). In addition, weaker modes with higher $k_{||}$ are also excited.

The measured dispersion diagram can be further used to investigate the details of the LT_1 resonances by extracting the amplitude values $[A_{LT_1}(f)]$ along a single dispersion curve (see Fig. 3). The dispersion diagram presents a decomposition of the measured wave motion to the different eigenmodes at each frequency, and therefore, by following a single dispersion curve, the contribution of those particular eigenmodes can be isolated and further investigated.

The electrical behavior of a multimode resonator is often presented with a modified Butterworth van Dyke equivalent circuit with several resonance legs.¹⁹ There is a mechanical analog to the electrical circuit, where the current drawn by the circuit is proportional to the mechanical vibration amplitude, and can be expressed as

$$I(\omega) = j\omega C_0 V + \sum_{p=1}^N \underbrace{\frac{k_p^2}{1 - k_p^2} C_0 Q_p \omega_p V}_{A_p} \underbrace{\frac{1}{1 + \frac{Q_p(\omega_p^2 - \omega^2)}{j\omega_p \omega}}}_{F_m(\omega)}, \quad (1)$$

where C_0 is the static capacitance, a resonator-geometry-related constant that is independent of the eigenmode p , V is the driving voltage, k_p the electromechanical coupling coefficient, Q_p the quality factor and ω_p the angular resonance frequency of the eigenmode p . The shape of the resonance peak is determined by the part labeled $F_m(\omega)$, whereas the part A_p is a mode-dependent constant. To demonstrate the extraction of the parameters, the properties of the 6 first eigenresonances of the LT_1 dispersion curve are determined by fitting Eq. (1) to the extracted LT_1 amplitude data, keeping the first term as a free offset parameter B_{offset} .

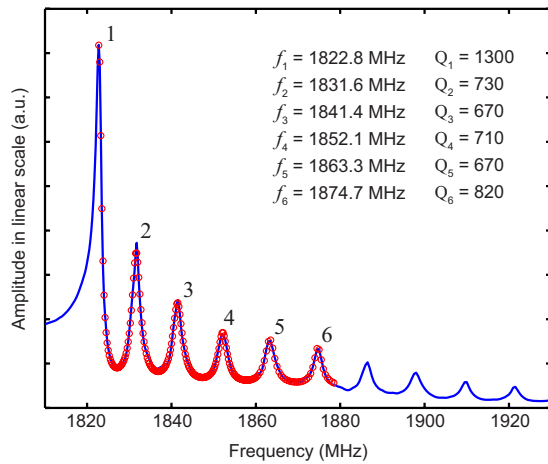


FIG. 3. (Color online) Extracted vibration amplitudes A_{LT_1} along the LT_1 dispersion curve as a function of frequency (solid line), along with the results of the mechanical equivalent circuit model fitted to the 6 first eigenmodes (circles). The resulting eigenfrequencies and Q -values are presented as an inset. There is an excellent correspondence between the extracted mechanical response and the function fit, indicating that the LT_1 dispersion curve may be described as a sum of a discrete set of independent eigenmodes.

$$M(\omega) = B_{\text{offset}} + \sum_{p=1}^6 A_p \frac{1}{1 + \frac{Q_p(\omega_p^2 - \omega^2)}{j\omega_p\omega}}. \quad (2)$$

The resulting resonance frequencies f_p and values of Q_p are shown along with the original data [$A_{LT_1}(f)$, solid line] and the function fit (circles) in Fig. 3. The measured amplitude distributions corresponding to the 6 first LT_1 eigenfrequencies are shown in Fig. 2.

There is an excellent correspondence between the LT_1 amplitude line profile extracted from the dispersion curves and the fitted $M(\omega)$, validating the equivalent circuit based representation of the multimode resonator. It is to be noted that the left-hand-side of the first peak in Fig. 3 lies below the cutoff frequency of the LT_1 mode, where the vibration consists of mainly forced $|k_{||}| \approx 0$ vibration, whereas the right hand side is above the cutoff, where lateral propagation is possible. This explains the asymmetric shape of the first peak. The approximate Q -value of $Q > 1100$ of the main resonance determined from the electrical frequency response corresponds well to the Q -value of 1300 obtained via the interferometer measurements. The Q -values of the following resonances ($Q_2 - Q_6$) range from 670 to 820, which is clearly lower than that for the main resonance. The Q -values of the individual lateral resonances are affected by several loss mechanisms, such as electrical and viscous losses, acoustic leakage laterally and through the reflector, etc. A deeper analysis of these effects is beyond the scope of this letter.

The acoustic wave fields excited in a 1820 MHz AlN solidly mounted BAW resonator were measured in detail. The discrete set of lateral eigenmodes excited in the resona-

tor is seen in the measured dispersion curve as a chain of maxima rather than as a continuous mode branch. Following a measured dispersion curve enables us to determine the properties of the individual eigenmodes (resonances) by fitting a mechanical response function to the measured vibration data. This approach facilitates direct experimental extraction of the eigenfrequencies, Q -values, and relative strengths of these resonances. The relative strengths of the coupling coefficients, k_p , are available from the model through the A_p parameter, but obtaining their absolute values would require exact knowledge of the relation between the mechanical amplitude and the resonator current and leads to considerations beyond the scope of this letter. This direct characterization of the LT_1 eigenmodes yields valuable information on the underlying device physics and also feedback to the component designers.

K. Kokkonen thanks the Finnish Cultural Foundation and the Nokia Foundation for scholarships.

- ¹J. V. Knuutila, P. T. Tikka, and M. M. Salomaa, *Opt. Lett.* **25**, 613 (2000).
- ²J. E. Graebner, B. P. Barber, P. L. Gammel, S. Gopani, and D. S. Greywall, *Appl. Phys. Lett.* **78**, 159 (2001).
- ³G. G. Fattinger and P. T. Tikka, *Appl. Phys. Lett.* **79**, 290 (2001).
- ⁴K. L. Telschow, V. A. Deason, D. L. Cottle, and J. D. Larson, *IEEE Trans. Ultrason. Ferroelectr. Freq. Control* **50**, 1279 (2003).
- ⁵K. Kokkonen and M. Kaivola, *Appl. Phys. Lett.* **92**, 063502 (2008).
- ⁶T. Fujikura, O. Matsuda, D. M. Profunser, O. B. Wright, J. Masson, and S. Ballandras, *Appl. Phys. Lett.* **93**, 261101 (2008).
- ⁷K.-Y. Hashimoto, K. Kashiwa, T. Omori, M. Yamaguchi, O. Takano, S. Meguro, and K. Akahane, *Microwave Symposium Digest, 2008 IEEE MTT-S International*, 15–20 June, Atlanta, Georgia (IEEE, New Jersey, 2008), p. 854.
- ⁸J. D. Larson III, R. C. Ruby, and P. Bradley, U.S. Patent No. 6,215,375 B1, (10 April 2001).
- ⁹A. Link, E. Schmidhammer, H. Heinze, M. Mayer, B. Bader, and R. Weigel, *Microwave Symposium Digest, 2006 (IEEE, New Jersey, 2006)*, pp. 394–397.
- ¹⁰D. Rosén, J. Bjurström, and I. Katardjiev, *IEEE Trans. Ultrason. Ferroelectr. Freq. Control* **52**, 1189 (2005).
- ¹¹J. Kaitila, M. Ylilammi, J. Ellä, and R. Aigner, *Proc. - IEEE Ultrason. Symp.* **1**, 84 (2003).
- ¹²S. Marksteiner, J. Kaitila, G. G. Fattinger, and R. Aigner, *Proc. - IEEE Ultrason. Symp.* **1**, 329 (2005).
- ¹³G. G. Fattinger, S. Marksteiner, J. Kaitila, and R. Aigner, *Proc. - IEEE Ultrason. Symp.* **2**, 1175 (2005).
- ¹⁴J. E. Graebner, H. F. Safar, B. Barber, P. L. Gammel, G. J. Herbsommer, L. A. Fetter, J. Pastalan, H. A. Huggins, and R. E. Miller, *Proc. - IEEE Ultrason. Symp.* **1**, 635 (2000).
- ¹⁵G. G. Fattinger and P. T. Tikka, *IEEE MTT-S Int. Microwave Symp. Dig.* **1**, 371 (2001).
- ¹⁶T. Makkonen, T. Pensala, J. Vartiainen, J. V. Knuutila, J. Kaitila, and M. M. Salomaa, *IEEE Trans. Ultrason. Ferroelectr. Freq. Control* **51**, 42 (2004).
- ¹⁷K. L. Telschow and J. D. Larson, *Proc. - IEEE Ultrason. Symp.* **1**, 280 (2003).
- ¹⁸J. Meltaus, T. Pensala, and K. Kokkonen, *Proc. - IEEE Ultrason. Symp.* **1**, 1544 (2008).
- ¹⁹B. A. Auld, *Acoustic Fields and Waves in Solids*, 2nd ed. (Robert E. Krieger, Malabar, FL, 1990), Vol. 2, pp. 260–261.